FEBS Letters 582 (2008) 1661–1666

A comparative metabolomic study of NHR-49 in *Caenorhabditis elegans* and PPAR-α in the mouse

Helen J. Atherton[a], Oliver A.H. Jones[a], Shahid Malik[b], Eric A. Miska[c], Julian L. Griffin[a,*]

[a] *The Department of Biochemistry, Tennis Court Road, University of Cambridge, Cambridge CB2 1QW, UK*
[b] *Chenomx, Suite 800, 10050 – 112 Street, Edmonton, Alberta T5K 2J1, Canada*
[c] *Wellcome Trust/Cancer Research UK Gurdon Institute, University of Cambridge, Tennis Court Road, Cambridge CB2 1QN, UK*

Received 19 March 2008; accepted 13 April 2008

Available online 22 April 2008

Edited by Laszlo Nagy

Abstract **Proton Nuclear Magnetic Resonance spectroscopy and Gas Chromatography Mass Spectrometry based metabolomics has been used in conjunction with multivariate statistics to examine the metabolic changes in *Caenorhabditis elegans* following the deletion of nuclear hormone receptor-49 (*nhr-49*). Deletion of the receptor produced profound changes in fatty acid metabolism, in particular an increase in the ratio of unsaturated to saturated fatty acids, a decrease in the concentration of glucose and increases in lactate and alanine. Given the proposed functional similarity between *nhr-49* and the mammalian peroxisome proliferator-activated receptors (PPARs) these changes were compared with the metabolome of the PPAR-α null mouse. The metabolomic approach demonstrated a number of similarities including the regulation of lipid synthesis, β-oxidation of fatty acids and changes in glycolysis/gluconeogenesis.**

Keywords: Peroxisome proliferator-activated receptors; Functional genomics; Nuclear hormone receptors; NMR spectroscopy; Gas chromatography mass spectrometry

1. Introduction

The nematode worm *Caenorhabditis elegans* is an ideal tool for functional genomics. It has been characterised in great detail in terms of its development, morphology and physiology at the cellular level and its genome has been completely sequenced [1]. A powerful genetic toolset for *C. elegans* is available and a large collection of mutants are available. In addition, *C. elegans* is one of the few animals for which high-throughput in vivo RNA interference (RNAi) screening has been established [2]. Many of the genes involved in human disease, including those involved in diabetes and obesity, have homologues in *C. elegans* and their study has made a large contribution to our current understanding of the gene pathways involved in human disease.

In functional genomic studies of yeast, Raamsdonk and colleagues suggested an approach based on metabolomics to reveal the phenotypes of silent mutations [3]. This has been further demonstrated in the excreted metabolites produced by yeast ('metabolic footprinting'; [4]). In a similar manner, metabolomics has been shown to be highly discriminatory for a variety of mutants in different organisms including *Arabidopsis* [5] and mice [6].

In this study we have examined the metabolome of *C. elegans* using a combination of ^{1}H Nuclear Magnetic Resonance (NMR) spectroscopy to examine aqueous soluble metabolites and Gas Chromatography Mass Spectrometry (GC–MS) to examine the total fatty acid composition. These tools have been used in conjunction with multivariate statistics to examine the role of *nhr-49*. Whilst this nuclear hormone receptor has significant homology with hepatocyte nuclear factor 4 (*HNF4*) in mammals, Van Gilst and colleagues have proposed the function is closer to the mammalian peroxisome proliferator-activated receptors (PPARs) [7,8]. The metabolic phenotype of *C. elegans nhr-49* mutants has therefore been compared with the metabolic changes in the PPAR-α null mouse in order to demonstrate the translational potential of metabolomics-based functional genomics.

2. Methods

2.1. Nematode methods

C. elegans was grown using standard conditions at 20 °C on plates seeded with *Escherichia coli* strain OP50 [9]. The wild-type strain was var. Bristol *N*2 [10]. The *nhr-49* mutant strain used was VC870 (*nhr-49*(gk405)), which was generated by the *C. elegans* knockout consortium [11] and distributed by the *Caenorhabditis* Genetics Center, University of Minnesota, Twin Cities, MN. For each experiment approximately 2000 mixed-stage animals were harvested and nine repeats were made. The animals were washed twice in double distilled H_2O, centrifuged (2000 rpm, 20 min) and the worm pellets were stored at −80 °C until extraction.

2.2. Mouse husbandry

Tissues from SVEV/129 mice, and PPAR-α null mice ($n = 5$; 5 months of age) were obtained from stable colonies at the University of Oxford. The UK Home Office approved all procedures. Mice were fed standard laboratory chow ad libitum prior to death (Special Diet Services, Essex, UK). Animals were killed by terminal anaesthesia and livers were collected within 30 s. All livers were stored at −80 °C until extraction.

2.3. Metabolite extraction

Metabolites from mouse liver tissue or whole nematodes were extracted using a methanol–chloroform extraction procedure. Frozen tissue (~100 mg) was pulverised with dry ice, 600 μl of a methanol–chloroform mix (2:1 v:v) was added and samples were sonicated for 15 min. Two hundred microliters each of chloroform and water were

*Corresponding author. Fax: +44 0 1223 333 345.
E-mail address: jlg40@mole.bio.cam.ac.uk (J.L. Griffin).

0014-5793/$34.00
doi:10.1016/j.febslet.2008.04.020

then added, and the samples centrifuged. The aqueous layer was dried overnight in an evacuated centrifuge and the lipid fraction was dried overnight under nitrogen.

2.4. High resolution ^1H NMR spectroscopy of aqueous fraction

The dried extracts were rehydrated in 600 μl D_2O, buffered in 0.24 M sodium phosphate (pH 7.0) containing 1 mM (sodium-3-(tri-methylsilyl)-2,2,3,3-tetradeuteriopropionate (TSP) (Cambridge Isotope Laboratories MA, USA) as an internal standard. The samples were analysed using an AVANCE II+ NMR spectrometer operating at 500.13 MHz for the ^1H frequency (Bruker, Germany) using a 5 mm TXI probe. Spectra were collected using a solvent suppression pulse sequence based on a one-dimensional NOESY pulse sequence to saturate the residual ^1H water signal (relaxation delay = 2 s, t_1 = 3 μs, mixing time = 150 ms, solvent presaturation applied during the relaxation time and the mixing time). One hundred and twenty-eight transients were collected into 16 K data points over a spectral width of 12 ppm at 27 °C. In addition, representative samples of nematodes were also examined by two-dimensional spectroscopy, including COSY (COrrelation SpectroscopY) and HSQC (Heteronuclear Single Quantum Coherence) spectroscopy [12], in conjunction with reference to previous literature and databases ([13,14]; Madison Metabolomics Consortium Database, http://mmcd.nmrfam.wisc.edu/index.html and the Chenomx spectral database contained in Chenomix NMR Suite 5.0 (Chenomx, Alberta, Canada)).

2.5. GC–MS of lipid fraction

Lipids were dissolved in 0.25 ml of chloroform/methanol (1:1 v/v). 100 μl BF_3/methanol (Sigma-Aldrich) was added and the vials were incubated at 80 °C for 90 min. 0.3 ml H_2O and 0.6 ml hexane was added and each vial vortex mixed. The organic layer was evaporated to dryness before reconstitution in 200 μl hexane for analysis.

The derivatised organic metabolites were injected onto a ZB-WAX column (30 m × 0.25 mm ID × 0.25 μm df; 100% polyethylene glycol). The initial column temperature was 60 °C and was held for 2 min. This was increased by 15 °C min^{-1} to 150 °C then increased at a rate of 4 °C min^{-1} to 230 °C. The column eluent was introduced into a Trace DSQ quadrupole mass spectrometer (Thermo Electron) (transfer line temperature = 240 °C, ion source temperature = 250 °C, electron beam = 70 eV). The detector was turned on after 240 s and data was collected in full scan mode using three scans s^{-1} across a mass range of 50–650 *m/z*.

2.6. Multivariate statistical analysis

NMR spectra were processed using ACD one-dimensional NMR processor (vers. 8, ACD, Toronto, Canada). Free induction decays were Fourier transformed following multiplication by a line broadening of 1 Hz, and referenced to TSP at 0.0 ppm. Spectra were phased and baseline corrected manually. Each spectrum was integrated using 0.04 ppm integral regions between 0.5 and 4.5, and 5.1–10.0 ppm. Each spectral region was normalised to a total integral value of 10000. In addition the Chenomx software was used to peak fit individual metabolites, and a dataset was produced consisting of these fitted resonances.

GC–MS Chromatograms were analysed using Xcalibur, version 2.0 (Thermo Fisher), integrating each peak individually. Each integrated peak was normalised so that the total sum of peaks was set to 10000. Deconvolution of overlapping peaks was achieved by traces of single ions. Mass spectra were assigned using the NIST database of mass spectra and standard compound analysis.

Datasets were imported into SIMCA-P 11.0 (Umetrics, Umeå, Sweden) for processing using principal components analysis (PCA) and partial least squares-discriminate analysis (PLS-DA; a regression extension of PCA used for supervised classification). GC–MS data was scaled to unit variance by dividing each variable by $1/(S_k)$ where S_k is the standard deviation of the variable. ^1H NMR spectroscopy data was Pareto scaled, in which each variable was centred and multiplied by $1/(S_k)^{1/2}$. Identification of major metabolic perturbations within the pattern recognition models was achieved by analysis of corresponding loadings plots, with metabolites selected which are considered to have a significant contribution to that PC ($p < 0.05$ following a jack knifing routine). Additionally, R^2 and Q^2 were used as measures for the robustness of a pattern recognition model. R^2 is the fraction of variance explained by a component, and cross validation of R^2 gives Q^2 which reveals the fraction of the total variation predicted by a component. In addition a leave-one-out analysis was performed on each *C. elegans* dataset to examine how well class membership was predicted.

3. Results

Fig. 1a shows a high resolution ^1H NMR spectrum acquired in ~14 min of the aqueous metabolites extracted from *C. elegans*. Using the library and peak fitting routine within the Chenomx NMR Suite 5.0 software package, a total of 55 metabolites were identified and quantified, and confirmed by the use of two-dimensional NMR spectroscopy (Fig. 1b and c) and GC–MS [Supplementary Table 1 and Fig. 1].

Using a bucketing routine to integrate the NMR spectra and applying PLS-DA to the resultant dataset, classification into wild-type and *nhr-49* mutants was achieved (Fig. 2a; Supplementary Fig. 2a). Using a leave one out analysis of the data set all samples except one were accurately predicted to belong to the correct group. On inspection this sample belonged to a spectrum with a low signal to noise ratio. Examination of the loadings plots showed that the metabolites which were responsible for this classification were increases in lactate (δ 1.30–1.34, signifying the bucket represented in the loadings plot), alanine (δ 1.46–1.50), leucine (δ 1.62–1.66) and decreases in lysine (δ 2.98–3.06), glucose (δ 3.26–3.34; δ 3.50–3.62), malonate (δ 3.10–3.14) and aspartate (δ 2.70–2.74) in the mutant worms.

Examination of the total fatty acid complement of *C. elegans* demonstrated that a total of 42 peaks were detected in the chromatogram, with 31 of these being identified through a combination of the NIST library and retention time matching of known standards [Supplementary Table 2 and Supplementary Fig. 1]. Applying PLS-DA to the integrated peaks of the chromatograms the two groups were separated across 2 PLS-DA components (Fig. 2b; Supplementary Fig. 2b). Using a leave-one-out analysis the class membership of all samples were correctly predicted, although two samples were identified as being outliers to the model according to the distance to model criteria. These samples contained high concentrations of palmitoleidic acid which is found in high concentrations within *E. coli,* and may relate to a higher proportion of *E. coli* to *C. elegans* in the agar lawn at sampling. Examining the loadings plots of the PLS-DAs for the fatty acid data set, the metabolites increased in the mutant nematodes were α-linolenic acid, arachidonic acid, non-adecanoic acid, dihomo-γ-linolenic acid (8,11,14-eicosatrienoic acid), heptadecenoic acid, γ-linolenic acid and docosanoic acid and there was a decrease in a branched chain form of palmitate. Using a Cooman's plot analysis the lipid profiles correctly predicted genotype for all samples (Supplementary Fig. 2c).

Metabolomic analysis of liver from the 5-month PPAR-α null mouse revealed a number of changes similar to those observed in the *nhr-49* mutant *C. elegans* strain. ^1H NMR spectroscopy of the aqueous soluble metabolites in conjunction with PLS-DA showed the PPAR-α null samples could be differentiated from age matched controls through an increase in lactate (δ 1.30–1.34), citrate (δ 2.54–2.58) and glutamate (δ 2.10–2.18, 2.34–2.38) and a decrease in glucose concentration (δ 3.38–3.42), (δ 3.72–3.76), (δ 3.90–3.94) and (δ 5.20–5.24) and taurine (δ 3.42–3.46; 3.26–3.30) ($R^2 = 0.88$, $Q^2 = 0.47$) (Fig. 2c). Similarly, PLS-DA of the fatty acid composition, following analysis by GC–MS, was able to distinguish PPAR-α

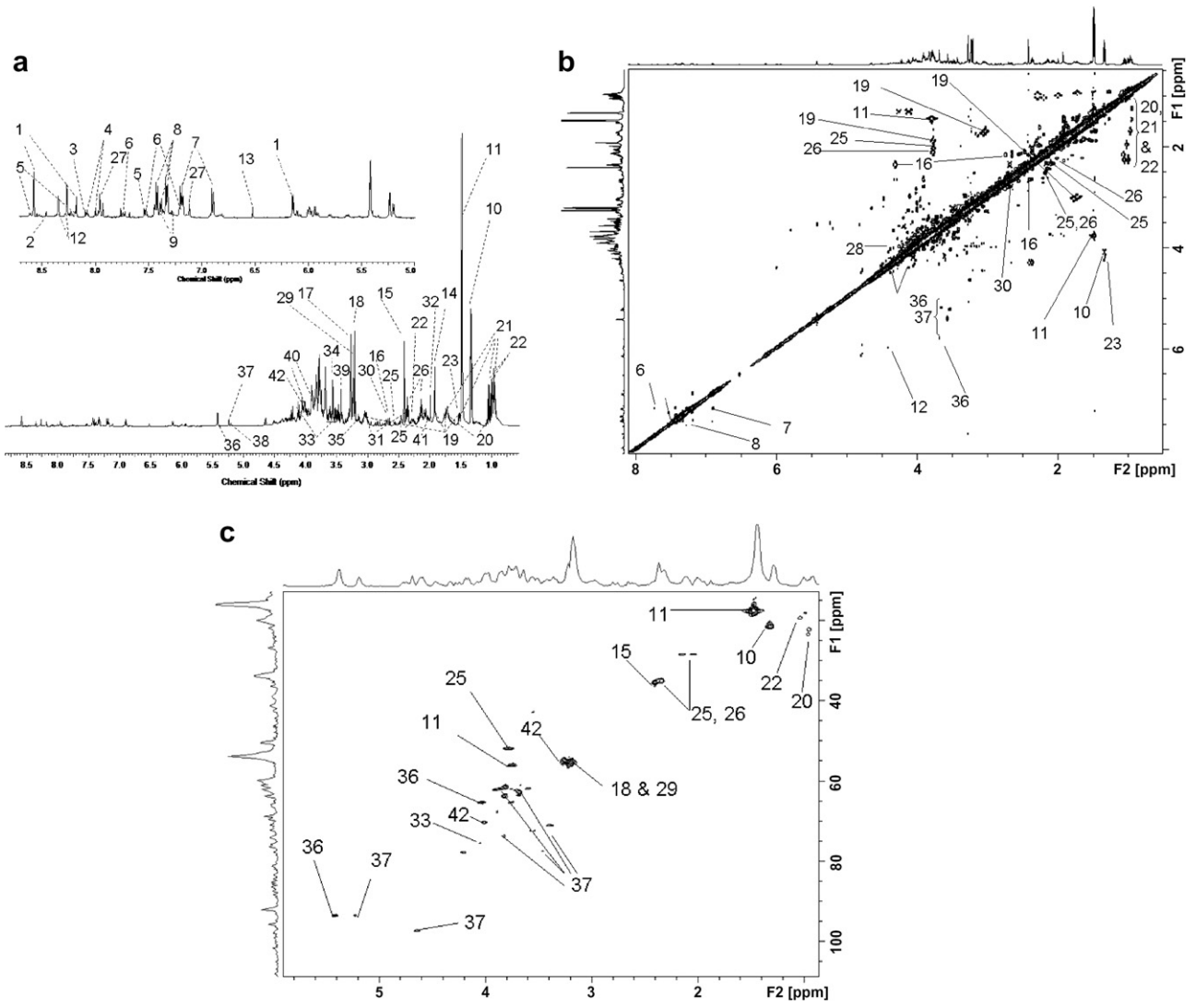

Fig. 1. (a) Annotated ^{1}H NMR spectrum showing aqueous soluble metabolites extracted from *C. elegans*. Assignments were confirmed through the use of COSY (b) and HSQC (c) spectra. Key: 1. ANP, 2. formate, 3. GTP, 4. hypoxanthine, 5. nicotinamide, 6. indoxyl sulphate, 7. 4-Hydroxyphenylacetic acid, 8. phenylalanine, 9. phenylacetylglycine, 10. lactate, 11 alanine, 12. inosine, 13. fumarate, 14. acetate, 15. succinate, 16, malate, 17. TMAO, 18. choline, 19 lysine, 20. leucine, 21. iso-leucine, 22. valine, 23. threonine, 24. beta-alanine, 25. glutamine, 26. glutamate, 27. histidine, 28. tyrosine, 29. phosphocholine, 30. aspartate, 31. alpha-ketoglutarate, 32. methionine, 33. myo-inositol, 34. glycine, 35. melonate, 36. glucose-6-phosphate, 37. glucose, 38. fructose, 39. methanol, 40. serine, 41. proline, 42. betaine. In addition there are numerous sugar and amino acid resonances between ~3.3 and 4.0 ppm.

null samples from controls by an increase in concentration of arachidonic acid, linoleic acid, eicosanoic acid, lauric acid, and di-homo-γ-linolenic acid (8,11,14-eicosatrienoic acid), and a decrease in concentration of palmitic acid, and a branched chain 16:0 fatty acid ($R^2 = 0.81$, $Q^2 = 0.25$; Fig. 2d).

To compare directly the mutants, PLS-DA models were constructed of the aqueous (NMR spectroscopy) and lipid phase (GC–MS) datasets. No model could be built that successfully separated mutants from wild-type for the combined NHR-49 and PPAR-α aqueous dataset, with this dataset being dominated by the differences between species. However, a comparison of the loadings for the different PLS-DA plots that distinguished mutant from wild-type for the aqueous extracts demonstrated some marked similarities, and in particular that both mutants had a decreased concentration of glucose and increased concentration of lactate (Fig. 2e). Using PLS-DA to analyse all the lipid extracts, separation was detected in PLS-DA component 1 according to species ($R^2(X) = 64\%$; $R^2(Y) = 32\%$; $Q^2 = 27\%$) and according to mutant/wild-type status in PLS-DA component 2 ($R^2(X) = 17\%$; $R^2(Y) = 15\%$; $Q^2 = 11\%$) (Fig. 2f). This separation was caused by a decrease in oleate and increases in arachidonic acid, eicosanoic acid and di-homo-γ-linolenic acid in the mutants (Fig. 2g).

4. Discussion

In this study we have demonstrated the versatility of a combined high resolution ^{1}H NMR spectroscopy and GC–MS based profiling approach to study metabolic changes in *C. elegans*. The approach detected and quantified ~100 metabolites of which 86 were identified. Both approaches are rapid and cheap on a per sample basis, indicating they could be used as a rapid screening tool of *C. elegans* mutants. The metabolic

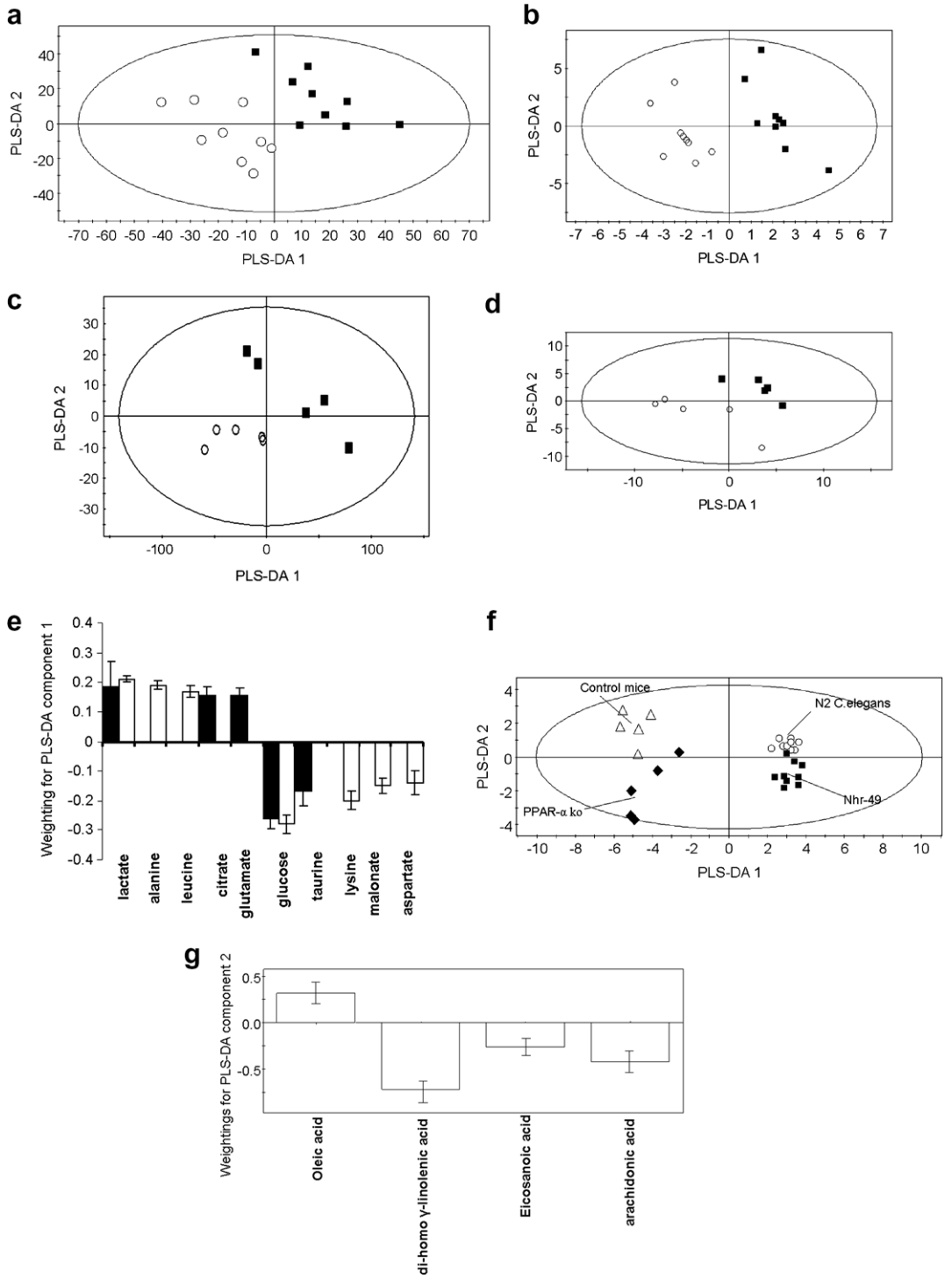

Fig. 2. Score plots showing the differentiation of *nhr-49* (○) and *N*2 control *C. elegans* nematodes (■) following (a) PLS-DA of the aqueous soluble metabolites by ^{1}H NMR spectroscopy ($R^2(X) = 38\%$; $R^2(Y) = 76\%$; $Q^2 = 54\%$) and (b) PLS-DA analysis of the total lipid compliment by GC–MS following methyl esterification ($R^2(X) = 54\%$, $R^2(Y) = 92\%$; $Q^2 = 76\%$). (c) PLS-DA score plots showing the differentiation of PPAR-α null tissue (○) and control tissue (■) following analysis of the aqueous soluble metabolites by ^{1}H NMR spectroscopy, and (d) following PLS-DA analysis of the total lipid composition by GC–MS following methyl esterification. (e) A comparison of the loadings for PLS-DA 1 from the scores plots displayed in (a) and (c) demonstrating a number of similarities between the two PLS-DA plots. Positive values indicate an increase in the mutant (black bars are mice, white bars are *C. elegans*). The error bars were derived from jack knifing to determine the leverage each variable had on the PLS-DA component. Where no bar is shown for a metabolite this metabolite did not change significantly in concentration as judged by the jack knifing routine. (f) PLS-DA plot comparing the total lipid composition for both mutant models. Key: *nhr-49* (■) and *N*2 control *C. elegans* nematodes (○); PPAR-α null tissue (♦) and control mouse tissue (Δ) (g) coefficients of the major components contributing to PLS-DA 2 of the scores plot in (f) which separated mutants from wild-types. The error bars were derived from jack knifing to determine the leverage each variable had on the PLS-DA component. A positive value indicates a decrease in mutant animals. Only variables where the weightings were significantly different from zero as determined by the jack-knifing procedure are included.

changes in *C. elegans nhr-49* mutants have been compared with the PPAR-α null mouse, demonstrating the metabolic similarity of the consequences for the loss of these genes in the two different species.

Previous studies looking at metabolism in the PPAR-α null mouse during fasting have described a significant reduction in fatty acid metabolism via β oxidation which has been attributed to a loss of regulation of genes that encode enzymes critical to this pathway [15], while we have previously detected a milder phenotype in fed animals [16]. In this study, we observed an increase in linoleic and di-homo-γ-linolenic acid (8,11,14-eicosatrienoic acid) in PPAR-α null livers and similar changes were observed in the *nhr-49* mutant nematodes with an increases in concentration of di-homo-γ-linolenic acid (8,11,14-eicosatrienoic acid), α-linolenic and γ-linolenic acid. This was further demonstrated by a combined analysis suggesting that *nhr-49* and PPAR-α have similar roles in the regulation of metabolism. These fatty acids are precursors for arachidonic acid, with the expression of the desaturases and elongase involved in this pathway being under PPAR-α control in mice and *nhr-49* control in *C. elegans*. These changes are also in keeping with the Q-PCR analysis performed by Van Gilst et al. [7] who detected decreased expression of fat-5, fat-6 and fat-7 (three Δ9-desaturases) transcripts involved in desaturation/elongation and acyl CoA synthetase (*acs-2*) and trifunctional enzyme (*ech-1*). Comparing these to known PPAR-α targets in mammals (e.g. http://www.genome.jp/dbget-bin/get_pathway?org_name=mmu&mapno=03320), both receptors target Δ9-desaturases and acyl-CoA synthetases.

One notable difference between our present study and that of Van Gilst et al. [7] examining the *nhr-49* mutant was that we detected no change in stearate, despite a marked increase being detected in the previous study. Similar increases in stearate have been detected in *fat-7* (F10D2.9; homologous with mammalian stearoyl-CoA desaturase and induced by *nhr-49*) and *nhr-80* mutants [7,17]. However, stearate also increases during fasting and the expression of *fat-7* varies markedly during development and fasting, suggesting that the concentration of stearate may be highly variable according to the physiological and developmental state of the nematodes, particularly in a colony of mixed stage animals. Despite, no alteration in the concentration of stearate being detected, the concentration of oleate was found to be significantly reduced in the mutant nematodes (Fig. 2g), a finding consistent with a reduction in the expression of Δ9-desaturase. Van Gilst et al. [7] reported that the expression of Δ9-desaturase (which converts stearate to monounsaturated oleate) was significantly decreased by *nhr-49* deletion. Oleate was also significantly reduced in the PPAR-α null livers (Fig. 2g), thus providing further evidence that NHR-49 and mammalian PPAR-α may have similar regulatory effects on the pathways of lipid metabolism.

In the *nhr-49* nematodes the perturbation in fat metabolism was accompanied by a decrease in glucose and an increase in lactate and alanine, indicative of an increase in the relative ratio of glycolysis to gluconeogenesis. Similar changes were also detected in the liver tissue of PPAR-α knock out mice in this study and in younger animals [16]. In mice, PPAR-α is known to control pyruvate dehydrogenase kinase 4 (PDK4) activity, and this can limit flux through the Krebs cycle by inhibiting pyruvate dehydrogenase [18]. Loss of PPAR-α prevents PDK4 expression, and this may lead to an active form of pyruvate dehydrogenase in the liver causing increased glucose utilisation. A similar interaction may exist between *nhr-49* and PDK in nematodes. Another plausible hypothesis is that there may be reduced flux through the glycolylate pathway arising from a decrease in precursor fatty acid β oxidation products, in particular acetyl Co-A, decreasing glucose synthesis.

In conclusion, our combined metabolomic approach suggests that *nhr-49* has a role in regulating lipid synthesis, β-oxidation of fatty acids, glycolysis and gluconeogenesis in a similar manner to the role of PPAR-α in the mouse liver.

Acknowledgements: This study was supported by Grants from the Biotechnology and Biological Sciences Research Council and Selcia (H.J.A. and J.L.G.), and the European Union (FP6 Contract No. 003956 (O.A.H.J.)). J.L.G. is a Royal Society (UK) University Research Fellow. E.A.M. was supported by a Programme Grant from Cancer Research UK. We would like to thank Rob Shaw for help with *C. elegans* husbandry.

Appendix A. Supplementary data

Supplementary data associated with this article can be found, in the online version, at doi:10.1016/j.febslet.2008.04.020.

References

[1] The *C. elegans* Sequencing Consortium (1998) Genome sequence of the nematode *C. elegans*: a platform for investigating biology. Science 282, 2012–2018.
[2] Kamath, R.S., Fraser, A.G., Dong, Y., Poulin, G., Durbin, R., Gotta, M., Kanapin, A., Le Bot, N., Moreno, S., Sohrmann, M., Welchman, D.P., Zipperlen, P. and Ahringer, J. (2003) Systematic functional analysis of the *Caenorhabditis elegans* genome using RNAi. Nature 421, 231–237.
[3] Raamsdonk, L.M., Teusink, B., Broadhurst, D., Zhang, N., Hayes, A., Walsh, M.C., Berden, J.A., Brindle, K.M., Kell, D.B., Rowland, J.J., Westerhoff, H.V., van Dam, K. and Oliver, S.G. (2001) A functional genomics strategy that uses metabolome data to reveal the phenotype of silent mutations. Nat. Biotechnol. 19, 45–50.
[4] Allen, J., Davey, H.M., Broadhurst, D., Heald, J.K., Rowland, J.J., Oliver, S.G. and Kell, D.B. (2003) High-throughput classification of yeast mutants for functional genomics using metabolic footprinting. Nat. Biotechnol. 21, 692–696.
[5] Fiehn, O., Kopka, J., Dormann, P., Altmann, T., Trethewey, R.N. and Willmitzer, L. (2000) Metabolite profiling for plant functional genomics. Nat. Biotechnol. 18, 1157–1161.
[6] Jones, G.L., Sang, E., Goddard, C., Mortishire-Smith, R.J., Sweatman, B.C., Haselden, J.N., Davies, K., Grace, A.A., Clarke, K. and Griffin, J.L. (2005) A functional analysis of mouse models of cardiac disease through metabolic profiling. J. Biol. Chem. 280, 7530–7539.
[7] Van Gilst, M.R., Hadjivassiliou, H., Jolly, A. and Yamamoto, K.R. (2005) Nuclear hormone receptor NHR-49 controls fat consumption and fatty acid composition in *C. elegans*. PLoS Biol. 3, e53.
[8] Van Gilst, M.R., Hadjivassiliou, H. and Yamamoto, K.R. (2005) A *Caenorhabditis elegans* nutrient response system partially dependent on nuclear receptor NHR-49. Proc. Natl. Acad. Sci. USA 102, 13496–13501.
[9] Wood, W.B. (1988) The Nematode *Caenorhabditis elegans*, Cold Spring Harbor Press, New York.
[10] Brenner, S. (1974) The genetics of *Caenorhabditis elegans*. Genetics 77, 71–94.
[11] Edgley, M., D'Souza, A., Moulder, G., McKay, S., Shen, B., et al. (2002) Improved detection of small deletions in complex pools of DNA. Nucleic Acids Res. 30, e52.
[12] Braun, S., Kalinowski, H.-O. and Berger, S. (1996) 100 and More Basic NMR Experiments: A Practical Course, VCH, Weinheim.

[13] Bundy, J.G., Osborn, D., Weeks, J.M., Lindon, J.C. and Nicholson, J.K. (2001) An NMR-based metabonomic approach to the investigation of coelomic fluid biochemistry in earthworms under toxic stress. FEBS Lett. 500, 31–35.
[14] Bundy, J.G., Spurgeon, D.J., Svendsen, C., Hankard, P.K., Osborn, D., Lindon, J.C. and Nicholson, J.K. (2002) Earthworm species of the genus Eisenia can be phenotypically differentiated by metabolic profiling. FEBS Lett. 521, 115–120.
[15] Reddy, J.K. and Hashimoto, T. (2001) Peroxisomal beta-oxidation and peroxisome proliferator-activated receptor alpha: an adaptive metabolic system. Annu. Rev. Nutr. 21, 193–230.
[16] Atherton, H.J., Bailey, N.J., Zhang, W., Taylor, J., Major, H., Shockcor, J., Clarke, K. and Griffin, J.L. (2006) A combined ^{1}H NMR spectroscopy- and mass spectrometry-based metabolomic study of the PPAR-alpha null mutant mouse defines profound systemic changes in metabolism linked to the metabolic syndrome. Physiol. Genom. 27, 178–186.
[17] Brock, T.J., Browse, J. and Watts, J.L. (2006) Genetic regulation of unsaturated fatty acid composition in *C. elegans*. PLoS Genet. 2, e108.
[18] Wu, P., Peters, J.M. and Harris, R.A. (2001) Adaptive increase in pyruvate dehydrogenase kinase 4 during starvation is mediated by peroxisome proliferator-activated receptor alpha. Biochem. Biophys. Res. Commun. 287, 391–396.